Quantum Electronics **46** (8) 743–748 (2016)

PHOTONIC-CRYSTAL STRUCTURES DOI: 10.1070/QEL16086

Defect modes of one-dimensional photonic-crystal structure with a resonance nanocomposite layer

S.G. Moiseev, V.A. Ostatochnikov

Abstract. **We have studied the defect modes of a structure of Fabry–Perot interferometer type, in which the layer separating Bragg mirrors is made of a heterogeneous composite material with metallic nanoscale inclusions. Effective optical characteristics of the nanocomposite material have resonance singularities in the visible region of the spectrum, which are conditioned by the surface plasmon resonance of metallic nanoparticles. It is shown that the spectral profile of the energy bandgap of the photonic structure can be modified by varying the volume fraction and size of nanoparticles. The interrelation of splitting and shift of defect modes with structural parameters of a nanocomposite layer is studied by means of a numerical–graphical method with allowance for the frequency dependences of phases and amplitudes of reflectances in Bragg mirrors.**

Keywords: *photonic crystal, defect modes, nanocomposite medium, plasmon resonance.*

1. Introduction

Photonic crystals, i.e. structures whose optical properties vary with a period comparable to the wavelength of electromagnetic radiation, are of great interest due to their unique electrodynamic characteristics [1, 2]. Electromagnetic waves propagating along the periodicity direction of a photonic-crystal structure undergo multiple re-reflections, which leads to the formation of a band structure in their spectrum. The presence of alternating regions of high and low transmission (reflection) in the spectrum is used for the development of new photonic and optoelectronic devices – photonic-crystal waveguides, Bragg filters, mirrors and resonators.

In a photonic crystal with a lattice defect (the structure's periodicity is disturbed), the transmission and reflection spectra are modified: in the region of a photonic bandgap, the structure transmits light in a certain narrow spectral band, which is called the defect band. The position and shape of the defect transmission band can be controlled by varying the geometric parameters of the defect layer [3–7]. On the basis of the defect photonic-crystal structures, new types of waveguides [8] and nanoresonators with a high Q-factor [9, 10] have been developed, and also new methods for increasing the intensity of nonlinear-optical processes [11, 12] have been proposed. New opportunities for controlling defect modes in a photonic crystal become available by using nanocomposite materials, optical characteristics of which substantially depend on their internal structure [13–18].

In this paper we consider a photonic structure with a nanocomposite defect layer formed on the basis of a dielectric medium, with metallic nanoparticles being uniformly distributed within its volume. The frequency and amplitude of the surface plasmon resonance of nanoparticles and, consequently, the effective characteristics of the nanocomposite layer depend on the dielectric constant of original materials, and also on the shape, size and concentration of nanoparticles [19–23]. The primary focus is on the study of modifications of the structure's photonic bandgap, revealing the mechanisms of splitting and shift of defect modes when varying the size and volume fraction of the composite nanoparticles.

2. Basic equations for photonic-crystal structures with a nanocomposite layer

Consider a one-dimensional photonic-crystal structure formed by plane-parallel layers of non-magnetic materials with dielectric constants ε_j ($j = 1, ..., N$). Let an electromagnetic wave propagate along the normal to the interface between the layers, i.e. along the stratification axis of the structure, coinciding with the z axis of the Cartesian coordinate system.

As applied to the structure under consideration, solving Maxwell's equations leads to two orthogonally polarised eigenwaves with the field components $E_x, H_y, 0$ and $H_x, E_y, 0$. Taking into account their proportionality to the factor $\exp(\mathrm{i}\omega t)$, we define the coordinate dependence of the field components for the first wave type in the following way:

$$E_{xj} = A_j \exp(-\mathrm{i}k_j z) + B_j \exp(\mathrm{i}k_j z), \quad H_{yj} = -\frac{\mathrm{i}}{k_0}\frac{\mathrm{d}E_{xj}}{\mathrm{d}z},$$

where A_j and B_j are the field amplitudes; $k_j = k_0\sqrt{\varepsilon_j}$ is the propagation constant; $k_0 = \omega/c$; and ω and c are the wave frequency and velocity in vacuum, respectively. We introduce a vector $\boldsymbol{F}_j$ with the components E_{xj} and H_{yj}, and a transfer matrix $\hat{m}_j$ which relates the wave field amplitude on the input and output surfaces of the jth layer:

$$F_j(z) = \hat{m}_j F_j(z + L_j),$$

S.G. Moiseev Ul'yanovsk State University, ul. L. Tolstogo 42, 432017 Ul'yanovsk, Russia; Ul'yanovsk Branch of Kotel'nikov Institute of Radio Engineering and Electronics, Russian Academy of Sciences, ul. Goncharova 48/2, 432011 Ul'yanovsk, Russia; Ul'yanovsk State Technical University, ul. Severny Venets 32, 432027 Ul'yanovsk, Russia; e-mail: serg-moiseev@yandex.ru;
V.A. Ostatochnikov Ul'yanovsk State University, ul. L. Tolstogo 42, 432017 Ul'yanovsk, Russia; Kazan Federal University, ul. Kremlevskaya 18, 420000 Kazan, Russia

Received 25 March 2016; revision received 16 May 2016
Kvantovaya Elektronika **46** (8) 743–748 (2016)
Translated by M.A. Monastyrskiy

where L_j is the layer thickness. In the case of normal incidence, the expression for the transfer matrix takes the form [24]

$$\hat{m}_j = \begin{pmatrix} \cos k_j L_j & -(\mathrm{i}/\sqrt{\varepsilon_j})\sin k_j L_j \\ -\mathrm{i}\sqrt{\varepsilon_j}\sin k_j L_j & \cos k_j L_j \end{pmatrix}. \quad (1)$$

Next we consider a structure representing two Bragg mirrors separated by an additional (defect) layer of the material. We assume that the mirrors are formed by the alternating layers of two different unabsorbing materials, with the sequence order of layers in one mirror being inverted relative to the other. The full transfer matrix of the structure under consideration is as follows:

$$\hat{Q} = (\hat{m}_1\hat{m}_2)^u \hat{m}_\mathrm{d} (\hat{m}_2\hat{m}_1)^v, \quad (2)$$

where the integer positive numbers u and v are equal to the numbers of binary layers (periods of the structure) in the Bragg mirrors; $\hat{m}_1$, $\hat{m}_2$ are the transfer matrices of the layers being a part of the dielectric mirrors; and $\hat{m}_\mathrm{d}$ is the transfer matrix of a layer separating the mirrors. The energetic coefficients of reflection and transmission for the entire structure placed into a dielectric medium with a refractive index n_e can be expressed in terms of elements of the matrix $\hat{Q}$ [24]:

$$R = \left| \frac{(Q_{11} + n_\mathrm{e}Q_{12})n_\mathrm{e} - (Q_{21} + n_\mathrm{e}Q_{22})}{(Q_{11} + n_\mathrm{e}Q_{12})n_\mathrm{e} + (Q_{21} + n_\mathrm{e}Q_{22})} \right|^2,$$
$$T = \left| \frac{2}{(Q_{11} + n_\mathrm{e}Q_{12})n_\mathrm{e} + (Q_{21} + n_\mathrm{e}Q_{22})} \right|^2. \quad (3)$$

The energetic absorption coefficient of the structure is calculated according to the formula $A = 1 - T - R$.

We assume that the approximation of the effective medium can be used to describe the optical properties of a nanocomposite layer placed between the photonic structure's mirrors. In the frame of this approximation, the separating layer corresponds to a transfer matrix of form (1), constructed for the effective (averaged over the macroscopic region) dielectric constant $\varepsilon_\mathrm{eff} = \varepsilon'_\mathrm{eff} + \mathrm{i}\varepsilon''_\mathrm{eff}$.

The effective medium models have been developed by Bruggeman, Maxwell Garnett, Landau and Lifshitz, et al. [25, 26] for nanocomposite structures of different topologies. In this paper we consider the heterogeneous structure of matrix type, which represents a dielectric (matrix), with metallic particles (inclusions) of spherical shape uniformly distributed within its volume. It is assumed that the proportion of metallic particles does not exceed a few percent of the total volume of material, which ensures a high transmission capacity of the composite layers, including the region of the plasmon resonance of particles, when the dissipative losses significantly increase. Effective optical characteristics of the matrix composites can be most adequately described by a relation of the Maxwell Garnet model:

$$\varepsilon_\mathrm{eff} = \varepsilon_\mathrm{m}\left[1 + \frac{3\eta(\varepsilon_\mathrm{p} - \varepsilon_\mathrm{m})}{3\varepsilon_\mathrm{m} + (1-\eta)(\varepsilon_\mathrm{p} - \varepsilon_\mathrm{m})}\right], \quad (4)$$

where η is the volume fraction of inclusions; and ε_m and ε_p are the dielectric constants of the matrix and inclusions, respectively (the magnetic permeabilities are set equal to unity). To characterise the nanocomposite material, we will use the effective complex refractive index $\sqrt{\varepsilon_\mathrm{eff}} = n_\mathrm{eff} + \mathrm{i}\varkappa_\mathrm{eff}$. It should be noted that the Maxwell Garnett approximation of the effective medium is applicable when the size of inhomogeneities is much smaller than the wavelength of the radiation used, i.e., in the optical range, the size of inclusions should not exceed a few tens of nanometers.

To describe the optical properties of metallic nanoparticles as part of the nanocomposite medium, we use an expression of the Drude model:

$$\varepsilon_\mathrm{p}(\omega) = \varepsilon_0 - \frac{\omega_\mathrm{p}^2}{\omega^2 + \mathrm{i}\omega\gamma}, \quad (5)$$

where ω_p is the plasma frequency of a free electron gas in an infinite volume; ε_0 describes the lattice contribution to the dielectric constant of the metal; and γ is the damping factor of plasma oscillations. Generally, the damping factor γ represents a size-dependent function for metal nanoparticles [26, 27]. The size effect occurs when the mean free path of conduction electrons exceeds the size of nanoparticles and the processes of electron scattering on the particle surface start to significantly contribute to the relaxation. Collisions of electrons with the nanoparticle surface are taken into account phenomenologically by introducing an additive to the relaxation rate, being inversely proportional to the particle radius:

$$\gamma(a) = \gamma_0 + q\frac{v_\mathrm{F}}{a}, \quad (6)$$

where γ_0 is the damping factor for an unrestricted volume of the metal; and v_F is the velocity of electrons at the Fermi energy. The proportionality factor q is determined by the details of the process of electron scattering on the surface of nanoparticles, and there is no versatile expression for that process. Commonly, the value of q is set equal to unity.

Note that, at the size of particle less than 1–2 nm, when the de Broglie wavelength of electrons becomes comparable to the size of the region of their localisation, the quantum size effects start to play a significant role, which also leads to a modification of the dielectric constant [27]. In this work we consider the case of nanoparticles with a diameter greater than 4 nm, for which the macroscopic description remains valid.

3. Spectral characteristics of a metal-dielectric nanocomposite and photonic-crystal structure mode

We investigate the resonance characteristics of the following systems: a single metallic nanoparticle, a volumetric array of nanoparticles (nanocomposite) and a one-dimensional resonator structure containing a nanocomposite layer in its structure. In our numerical calculations, a matrix of silicon dioxide (SiO_2) and inclusions of silver nanoparticles are considered for definiteness as composite medium components. Modern technologies allow matrix nanocomposites with various structural parameters to be formed on the basis of these materials [28–32].

The wavelength λ_p corresponding to the surface plasmon resonance of an individual metallic nanoparticle of spherical shape, embedded into a transparent dielectric matrix with a dielectric constant ε_m, is determined from the condition $\varepsilon'_\mathrm{p}(\lambda_\mathrm{p}) = -2\varepsilon_\mathrm{m}(\lambda_\mathrm{p})$ [33]. For a silver nanoparticle with parameters $\varepsilon_0 = 5$, $v_\mathrm{F} = 1.4\times10^6$ m s^{-1}, $\omega_\mathrm{p} = 1.36\times10^{16}$ s^{-1}, $\gamma_0 = 3.04\times10^{13}$ s^{-1} [34], the plasmon resonance in a matrix with $\varepsilon_\mathrm{m} = 2.25$ occurs at a wavelength $\lambda_\mathrm{p} \approx 420$ nm. The size effect manifests itself for

silver nanoparticles with a radius less than 5 nm and mainly leads to an increase in the real part of dielectric constant (5) and to a shift of the plasmon resonance of a nanoparticle to the long-wavelength region of the spectrum (due to the peculiarities of dispersion characteristics of silver). The size shift of the resonance wavelength is a few nanometers.

Resonance characteristics of a system of electrodynamically interacting particles differ from those of single particles, and this effect is the stronger the smaller is the average distance between them. To illustrate this fact, Figs 1 and 2 show the spectral dependences of real ($\varepsilon'_{\text{eff}}$) and imaginary ($\varepsilon''_{\text{eff}}$) parts of the dielectric constant of a nanocomposite, calculated using formulas (4)–(6) for different volume fractions and sizes of inclusions.

It is seen from Fig. 1 that a change in the size of inclusions (while maintaining their volume fraction) mainly affects the resonance amplitude. The particle size reduction degrades the Q-factor of the resonant system due to an increase in the damping parameter (6), which reduces the amplitude and increases the half-width of the resonance curves $\varepsilon'_{\text{eff}}(\lambda)$ and $\varepsilon''_{\text{eff}}(\lambda)$.

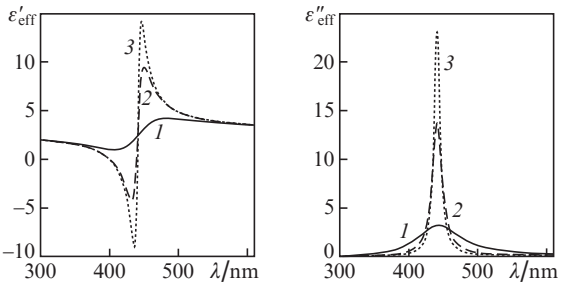

Figure 1. Dependences of the real ($\varepsilon'_{\text{eff}}$) and imaginary ($\varepsilon''_{\text{eff}}$) parts of the nanocomposite effective dielectric constant on the wavelength λ for nanoparticles with the radius a = (*1*) 2, (*2*) 10 and (*3*) 20 nm. The volume fraction of nanoparticles is $\eta = 0.1$.

Formulas (4) and (5) imply that detuning of the composite resonance from that of resonance of an isolated particle at $\omega_{\text{p}} \gg \gamma_0 + qv_{\text{F}}/a$ and relatively small values of the volume fraction of inclusions ($\eta \leqslant 0.1$) constitutes $\lambda_{\text{r}} - \lambda_{\text{p}} \approx \eta\lambda_{\text{p}}/2$, where λ_{r} is the composite's resonance wavelength. According to the above expressions, the resonance of the effective dielectric constant of a composite medium is always shifted relative

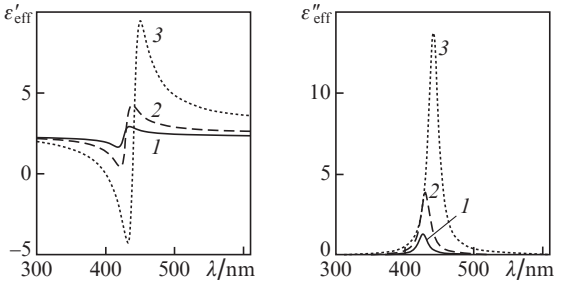

Figure 2. Dependences of the real ($\varepsilon'_{\text{eff}}$) and imaginary ($\varepsilon''_{\text{eff}}$) parts of the nanocomposite effective dielectric constant on the wavelength λ for the volume fraction of nanoparticles η = (*1*) 10^{-2}, (*2*) 3×10^{-2} and (*3*) 0.1. The nanoparticle radius is $a = 10$ nm.

to the resonance of a solitary particle into the long-wavelength region of the spectrum, while the detuning value is substantially dependent on the volume fraction of inclusions. This is confirmed by the dependences shown in Fig. 2.

In the nanocomposite case, the resonance wavelength shift may constitute tens of nanometers, which significantly exceeds the size detuning of the plasmon resonance for a solitary particle.

Next, we consider a resonant structure of Fabry–Perot interferometer type, representing a nanocomposite layer sandwiched between two dielectric Bragg mirrors. The maximum value of reflectivity of the mirrors is reached near the wavelength λ_{B} satisfying the Bragg condition of resonant reflection:

$$\lambda_{\text{B}} = \frac{2L_1}{l_1 - 1/2}\, n_1 = \frac{2L_2}{l_2 - 1/2}\, n_2, \tag{7}$$

where $L_{1,2}$ and $n_{1,2} = \sqrt{\varepsilon_{1,2}}$ are thicknesses and real refractive indices of the layers being a part of the mirrors; and $l_{1,2}$ are positive integers. The Fabry–Perot resonance condition for an unabsorbing structure is as follows:

$$\lambda_{0\text{d}} = \frac{2L_{\text{d}}}{l}\, n_{0\text{d}}, \tag{8}$$

where L_{d} is thickness of the layer separating the dielectric mirrors; $n_{0\text{d}} = n_{\text{d}}(\lambda_{0\text{d}})$ is the refractive index of the separating layer at the wavelength $\lambda_{0\text{d}}$; and $l = 1, 2, \ldots$ is the interference order. If the structure parameters are adjusted in such a way that the values of (7) and (8) are equal, the layered structure transmits light near the wavelength $\lambda = \lambda_{0\text{d}} = \lambda_{\text{B}}$ located in the region of the photonic bandgap of the mirrors, while reflection is suppressed (defect mode).

A defect mode can be split, which leads to the formation of multiple passbands within the photonic bandgap. One of the mechanisms of the mode splitting is associated with violation of the structure periodicity [35–37]. In the present work we investigate the splitting of the defect mode, caused by frequency dispersion of the dielectric constant of the medium filling the space between the resonator mirrors.

In papers [13, 14] the behaviour of defect modes when varying optical characteristics of the resonant layer is interpreted in the frame of the Fabry–Perot model using the resonance condition (8). However, the use of (8) in calculations of defect modes of the photonic structure with a resonant inclusion generally leads to inaccurate results, since this relation is formulated without considering the dependence of optical characteristics of Bragg structures on the radiation wavelength. Calculation of the wave number of a defect mode must be performed with allowance for the spectral dependences of the amplitudes and phases of the waves on all interfaces, including those located in the region of Bragg mirrors.

In the absence of absorption, the defect modes of a structure can be found from the condition of vanishing of the reflection coefficient [first equation in (3)]:

$$(Q_{11} + n_{\text{e}}Q_{12})n_{\text{e}} - (Q_{21} + n_{\text{e}}Q_{22}) = 0. \tag{9}$$

After transformation of equation (9) with regard to expressions (1) and (2), we obtain the condition for the defect mode ($u = v$) of the symmetric photonic structure placed into the medium with a refractive index $n_{\text{e}} = 1$:

$$m_{d12}(M_{11}^2 - M_{21}^2) - m_{d21}(M_{22}^2 - M_{12}^2) + 2m_{d11}(M_{11}M_{12} - M_{22}M_{21}) = 0, \quad (10)$$

where

$$m_{d11} = \cos\varphi_d, \quad m_{d21} = n_d^2 m_{d12} = -in_d \sin\varphi_d$$

are the transfer matrix elements for the central (defect) layer located between the dielectric mirrors;

$$M_{11} = \left(\cos^2\varphi - \frac{n_2}{n_1}\sin^2\varphi\right)U_{v-1}(\rho) - U_{v-2}(\rho);$$

$$M_{22} = \left(\cos^2\varphi - \frac{n_1}{n_2}\sin^2\varphi\right)U_{v-1}(\rho) - U_{v-2}(\rho);$$

$$M_{21} = n_1 n_2 M_{12} = -i(n_1 + n_2)\,U_{v-1}(\rho)\cos\varphi\sin\varphi;$$

$U_j(\rho) = \sin[(j+1)\arccos\rho]/\sqrt{1-\rho^2}$ are the Chebyshev polynomials of the second kind with respect to the variable $\rho = \cos^2\varphi - {}^1/_2(n_2/n_1 + n_1/n_2)\sin^2\varphi$; and $\varphi_d = (2\pi/\lambda)n_d L_d$ and $\varphi = (2\pi/\lambda)n_1 L_1 = (2\pi/\lambda)n_2 L_2 + \pi k$ ($k = 0, 1, 2, ...$) are the phase incursions in the central layer with a real refractive index n_d and in the layers of Bragg mirrors, respectively. The Fabry–Perot condition (8) represents a particular solution of equation (10).

Equation (10) allows one to determine a defect mode of the resonant structure with regard to virtually all factors (except for the dissipative losses): spectral dependences of the phase incursions, amplitudes and phases of reflection and transmission coefficients at the interfaces between different media, which are conditioned both by a change in the relationship between the wavelength and thickness of the layers and the refractive index dispersion. Because obtaining an analytical expression for the wavelength of the defect mode from equation (10) represents a non-trivial problem, the analysis of resonance conditions in the frame of this work is conducted by a numerical–graphical method.

The results of the numerical solution of equation (10) are shown in Figs 3 and 4 in the form of dependences $\delta n(\lambda) = [n_d(\lambda) - n_{0d}]/n_{0d}$. It is easy to see that the value of δn at the wavelength $\lambda_{0d} = \lambda_B$ takes the integer values satisfying the Fabry–Perot resonance condition (8): $\delta n(\lambda_{0d}) = 0, 1, 2, ...$ for a respective interference order $l = 1, 2, 3, ...$ The dielectric constants and thicknesses of the layers contained in the dielectric mirrors are hereafter selected as follows: $\varepsilon_1 = 2.25$ (SiO_2), $\varepsilon_2 = 5.52$ (TiO_2), $L_1 = 70$ nm, $L_2 = 44.7$ nm, which corresponds to the case of quarter-wave layers for a wavelength of $\lambda_B = 4L_1 n_1 = 4L_2 n_2 \approx 420$ nm. The number of binary layers in each mirror is equal to eight. The refractive index of the central layer at a wavelength of 420 nm is assumed to be equal to 1.5 ($n_{0d} = 1.5$), which coincides with the refractive index of the composite matrix n_m. The thickness of the layer separating the mirrors is $L_d = 140$ nm, which ensures fulfilment of the condition $\lambda_B = 2L_d n_m$.

Figures 3 and 4 also show the dispersion curves $\delta n_{eff}(\lambda) = [n_{eff}(\lambda) - n_m]/n_m$ for the nanocomposite materials differing in size and volume fraction of inclusions, calculated with the use of equations (4)–(6)

Obviously, total radiation transmission (reflection suppression) of the structure is attained at the points where the dispersion curve $\delta n_{eff}(\lambda)$ of the refractive index of the separating layer intersects the curves $\delta n(\lambda)$. If the parameters of mirrors are fixed, the number and coordinates of the intersection points are determined by the shape of the curve $\delta n_{eff}(\lambda)$. Ultimately, that means that the photonic structure's defect modes depend on the size and volume fraction of nanoparticles in the composite insert. In the case represented in Figs 3 and 4, the number of defect modes is equal to three, but this number may increase if the wings of the resonance curve $\delta n_{eff}(\lambda)$ would have intersection points with the curves $\delta n(\lambda)$ for the second ($l = 2$) and subsequent interference orders, which may occur, for example, when the concentration of inclusions increases. Note that in the case of small-size nanoparticles,

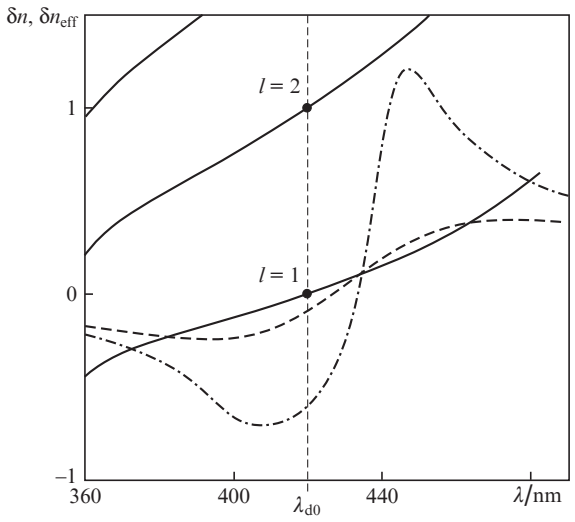

Figure 3. Photonic structure modes $\delta n(\lambda) = n_d(\lambda)/n_{0d} - 1$ (solid curves) obtained by numerical solution of equation (10), and dispersion curves $\delta n_{eff}(\lambda) = n_{eff}(\lambda)/n_m - 1$ for the nanocomposite material with a radius of nanoparticles $a = 2$ nm (dashed curve) and 10 nm (dot-and-dash curve). Here and in Fig. 4 bold dots show the values satisfying the Fabry–Perot resonance condition (8) for various interference orders l, while the vertical line corresponds to the wavelength $\lambda = 420$ nm. The volume fraction of nanoparticles is $\eta = 0.1$. The solution of equation (10) is obtained under conditions when energy dissipation in the nanocomposite layer is neglected.

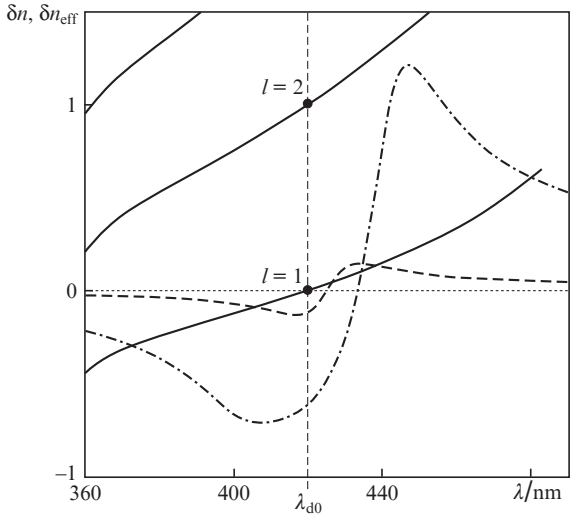

Figure 4. Photonic structure modes $\delta n(\lambda) = n_d(\lambda)/n_{0d} - 1$ (solid curves) obtained by numerical solution of equation (10), and dispersion curves $\delta n_{eff}(\lambda) = n_{eff}(\lambda)/n_m - 1$ for the volume fraction of nanoparticles $\eta = 10^{-4}$ (dotted line), 10^{-2} (dashed curve), and 10^{-1} (dot-and-dash curve). The nanoparticle radius is $a = 10$ nm.

the resonance curves are more flat (see Fig. 1), and, as a consequence, the number of intersection points with the curves $\delta n(\lambda)$ [the number of solutions of equation (10)] can be equal to unity.

It should be noted that absorption is always present in real metal-dielectric composites, which affects the amplitude of defect modes. As shown by the numerical analysis of the functions $R(\lambda)$ and $T(\lambda)$ (3) for real media, the losses in the composite layer generally lead to a change in the spectral shape and additional frequency shift of defect modes. The modification of defect modes in this case is stipulated by a change in the amplitude and phase characteristics of partial waves, refracted and reflected at the interfaces with a nanocomposite layer which is characterised by the effective refractive index with a non-zero imaginary part. Nevertheless, the numerical–graphical method presented above can also be applied to real structures with an absorbing separating layer, but in the conditions when the losses per one passage of the absorbing layer are relatively small, i.e. at $(2\pi/\lambda)\varkappa_d L_d \ll 1$, where $\varkappa_d$ is the extinction coefficient (the imaginary part of the complex refractive index) of the resonant layer.

4. Reflection and transmission spectra of the photonic-crystal structure with a resonant layer

Let us investigate the influence of the volume fraction and size of nanoparticles on the energy characteristics of a layered structure with the configuration and parameters given in the previous section of this paper. The reflection and transmission spectra of a photonic structure, calculated using expressions (1)–(3), are presented in Figs 5 and 6.

At a low volume fraction of nanoparticles ($\eta \ll 10^{-3}$), any nanocomposite is almost identical, in regard to its optical characteristics, to its own dielectric matrix for all wavelengths:

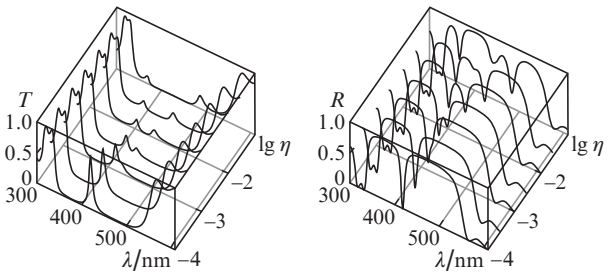

Figure 5. Transmittance T and reflectance R as functions of the wavelength λ and the volume fraction η of metallic nanoparticles. The nanoparticle radius is $a = 10$ nm. The structure parameters are given in the text.

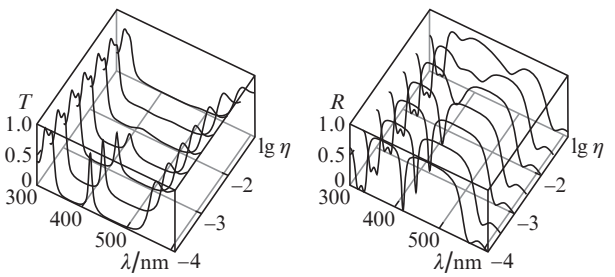

Figure 6. Same as in Fig. 5, but for the nanoparticle radius $a = 2$ nm.

$\varepsilon_{eff}(\lambda) \approx \varepsilon_m = \text{const}$, i.e. $\delta n_{eff}(\lambda) \approx 0$. As is seen from Figs 3 and 4, there is only one intersection point for $\delta n_{eff} = 0$. In this case, a single defect mode emerges in the photonic bandgap.

With increasing volume fraction of inclusions ($\eta \sim 10^{-2}-10^{-3}$) , the difference in dispersion characteristics of the composite medium and matrix material is increased, which is most noticeable in the plasmon resonance region of particles (see Fig. 2). An increase in the resonance amplitude $n_{eff}(\lambda)$ generally leads to an increase in the number of solutions of equation (10) from one to three (see Fig. 4). This leads to splitting of defect modes, herewith the frequency shifts between the central and lateral modes turn out the stronger the greater is the volume fraction of nanoparticles in the composite insert.

Splitting of modes is clearly seen in Fig. 5, which corresponds to the case of particles having a radius of 10 nm. However, only two extreme modes out of the three possible ones are observed in this case, since the central mode frequency is close to the plasmon resonance frequency, and therefore this mode is efficiently absorbed by the nanocomposite layer. It should be noted that the particle size has a significant impact on the number of defect modes in the spectra of the structure. For example, in the case of nanoparticles with a radius of 2 nm, a single defect mode is formed (Figure 6). As mentioned above, this is due to a more flat shape of the resonance curve $\delta n_{eff}(\lambda)$, which corresponds to a unique root of equation (10).

In the case of a nanocomposite layer with a relatively large fraction of inclusions ($\eta > 10^{-2}$), the dissipative losses and modification of the amplitude–phase characteristics of reflection from the resonance layer interfaces affect significantly the formation of the spectrum of the photonic structure. An increase in the concentration and a decrease in the size of nanoparticles lead to an increase in the dissipative losses in the composite layer and, as a result, to smoothing the lines of defect modes in the transmission spectrum. Thus, if the defect mode corresponds to the region of resonance absorption in the nanocomposite, it can be completely suppressed in the transmission spectrum [see $T(\lambda)$ in Fig. 6]. With increasing volume fraction of inclusions, the spectral width of the plasmon resonance increases, which causes a shift of defect modes toward the edges of the photonic bandgap of the structure (this fact is well illustrated by Fig. 5).

5. Conclusions

In the present study, we have investigated the spectral characteristics of a one-dimensional photonic-crystal structure, one of the layers of which possesses the resonance properties. The resonant layer is made of a nanocomposite material, with metallic nanoparticles possessing plasmon resonance in the optical spectrum range. These results are obtained on the basis of the transfer matrix method and approximation of the effective medium.

The layered structure we have considered is similar to the Fabry–Perot interferometer, in which a role of the layer separating the dielectric mirrors is played by a heterogeneous nanocomposite having the properties of a strongly dispersive medium with an absorption peak in the region of plasmon resonance inclusions. Optical characteristics of the nanocomposite, in particular the resonant frequency of the effective dielectric constant are determined by the size and volume fraction of metallic inclusions. Because of this, a change in the nanocomposite structural parameters results in a modifica-

tion of the defect modes of the photonic-crystal structure. It is shown that varying the volume fraction and nanoparticle size causes the splitting and shift of the structure modes near the nanocomposite layer's resonance. Calculation of the spectrum of defect modes requires taking into account the spectral dependences of amplitudes and phases of all partial waves arising from reflections at the interfaces of the photonic structure, superposition of which results in the formation of the reflection and transmission spectra. In the case of small losses in the nanocomposite layer ($\varkappa_d \ll \lambda/(2\pi L_d)$), the defect modes can be found by means of numerical–graphical solution of equation (9).

Splitting and shift of defect modes are typical for photonic-crystal structures with a resonant layer of any nature. If a nanocomposite material is used, it becomes possible to control the spectral characteristics of photonic structures by varying the volume fraction, shape and size of nanoparticles. In this paper, a model of a nanocomposite medium based on silicon dioxide is considered. The nanocomposites with a glass matrix having a uniform distribution of metallic nanoparticles can be prepared, for example, by means of ion implantation [31, 32] or high-temperature melting of opals with implanted metallic nanoparticles (described, for example, in [38]). It should be noted that from the viewpoint of the theory laid down in this paper, the material of a nanocomposite matrix is of no principal importance (restrictions may only be imposed due to peculiarities of the technology of nanocomposite manufacturing), while the effect of the defect mode splitting may also be observed for other materials, provided that the thicknesses of photonic structure layers are chosen to ensure matching of the defect mode frequency with the nanocomposite plasmon resonance frequency. In practice, any light-transmitting material with a positive dielectric constant may be used as the nanocomposite matrix, i.e. a nanocomposite on the basis of gas (aerosol), liquid, or liquid-crystal media (colloidal systems), as well as any other solid medium, for example PMMA [39], can be applied.

Acknowledgements. This work was supported by the Ministry of Education and Science of the Russian Federation (Project No. 14.Z50.31.0015, Task No. 3.2202.2014/K), and by the Russian Foundation for Basic Research (Grant No. 15-07-08111).

References

1. Sakoda K. *Optical Properties of Photonic Crystals* (Berlin: Springer, 2005).
2. Joannopoulos J.D., Johnson S.G., Winn J.N., Meade R.D. *Photonic Crystals* (Princeton: Princeton University Press, 1995).
3. Yang Y.-C., Kee C.-S., Kim J.-E., et al. *Phys. Rev. E*, **60**, 6852 (1999).
4. Schmidtke J., Stille W., Finkelmann H. *Phys. Rev. Lett.*, **90**, 083902 (2003).
5. Kopp V.I., Genack A.Z. *Phys. Rev. Lett.*, **89**, 033901 (2002).
6. Shabanov A.V., Vetrov S.I., Karneev A.Y. *Pis'ma Zh. Eksp. Teor. Fiz.*, **80**, 206 (2004).
7. Gevorgyan A.H., Harutyunyan M.Z. *Phys. Rev. E*, **76**, 031701 (2007).
8. Zheltikov A.M. *Usp. Fiz. Nauk*, **170**, 1203 (2000).
9. Akahane Y., Asano T., Song B.-S., Noda S. *Nature*, **425**, 944 (2003).
10. Painter O., Lee R.K., Scherer A., et al. *Science*, **284**, 1819 (1999).
11. Shi B., Jiang Z.M., Zhou X.F., Wang X. *J. Appl. Phys.*, **91**, 6769 (2002).
12. Dolgov T.V., Maidykovskii A.I., Martem'yanov M.G., Fedyanin A.A., Aktsipetrov O.A. *Zh. Eksp. Teor. Fiz.*, **75**, 17 (2002).
13. Vetrov S.I., Avdeeva A.Y., Timofeev I.V. *Zh. Eksp. Teor. Fiz.*, **140**, 871 (2011) [*JETP*, **113** (5), 755 (2011)].
14. Vetrov S.I., Pankin P.S., Timofeev I.V. *Kvantovaya Elektron.*, **44**, 881 (2014) [*Quantum Electron.*, **44**, 881 (2014)].
15. Moiseev S.G., Ostatochnikov V.A., Sementsov D.I. *Kvantovaya Elektron.*, **42**, 557 (2012) [*Quantum Electron.*, **42**, 557 (2012)].
16. Moiseev S.G., Ostatochnikov V.A., Sementsov D.I. *Pis'ma Zh. Eksp. Teor. Fiz.*, **100**, 413 (2014) [*JETP Lett.*, **100** (6), 371 (2014)].
17. Vetrov S.Ya., Pyatnov M.V., Timofeev I.V. *Phys. Rev. E*, **90**, 032505 (2014).
18. Vetrov S.I., Pankin P.S., Timofeev I.V. *Opt. Spektrosk.*, **119**, 69 (2015).
19. Maxwell Garnett J.C. *Phil. Trans. Royal Soc. London. Ser. A*, 237 (1906).
20. Oraevskii A.N., Protsenko I.E. *Pis'ma Zh. Eksp. Teor. Fiz.*, **72**, 641 (2000).
21. Sukhov S.V. *Kvantovaya Elektron.*, **35**, 741 (2005) [*Quantum Electron.*, **35**, 741 (2005)].
22. Moiseev S.G. *Appl. Phys. A*, **103**, 775 (2011).
23. Moiseev S.G. *Izv. Vyssh. Uchebn. Zaved., Ser. Fiz.*, **52** (11), 7 (2009) [*Russ. Phys. J.*, **52** (11), 1121 (2009)].
24. Born M., Wolf E. *Principles of Optics* (Oxford: Pergamon Press, 1964; Moscow: Nauka, 1970).
25. Spanier J.E., Herman I.P. *Phys. Rev. B*, **61**, 10437 (2000).
26. Kreibig U., Vollmer M. *Optical Properties of Metal Clusters* (Berlin: Springer, 1995).
27. Khlebtsov N.G. *Kvantovaya Elektron.*, **38**, 504 (2008) [*Quantum Electron.*, **38**, 504 (2008)].
28. Simo A., Polte J., Pfänder N., Vainio U., Emmerling F., Rademann K. *J. Am. Chem. Soc.*, **134**, 18824 (2012).
29. Wang Dawei, Guo Shiju, Yin Sheng. *Opt. Eng.*, **42**, 3585 (2003).
30. Stookey S.D., Araujo R.J. *Appl. Opt.*, **7**, 777 (1968).
31. Stepanov A.L., Hole D.E., Townsend P.D. *J. Non-Cryst. Solids*, **260**, 65 (1999).
32. Stepanov A.L. *Rev. Adv. Mater. Sci.*, **26** (1-2), 1 (2010).
33. Maier S.A. *Plasmonics: Fundamentals and Applications* (Berlin: Springer Science & Business Media, 2007).
34. Yannopapas V., Modinos A., Stefanou N. *Opt. Quantum Electron.*, **34**, 227 (2002).
35. Bayindir M., Kural C., Ozbay E. *J. Opt. A: Pure Appl. Opt.*, **3**, S184 (2001).
36. Eliseeva S.V., Ostatochnikov V.A., Sementsov D.I. *Izv. Vyssh. Uchebn. Zaved., Ser. Fiz.*, **55**, 72 (2012).
37. Dadoenkova N.N., Zabolotin A.E., Lyubchanskii I.L., Lee Y.P., Rasing T. *J. Appl. Phys.*, **108**, 093117 (2010).
38. Gorelik V.S., Zlobina L.I., Troitskii O.A., Chanieva R.I. *Inorg. Mater.*, **45**, 785 (2009).
39. Muzalev P.A., Kosobudskii I.D., Kul'batskii D.M., Ushakov N.M. *Inorg. Mater.: Appl. Res.*, **3** (1), 40 (2012).